

Holographic optical tweezers for object manipulations at an air-liquid surface

Alexander Jesacher, Severin Fürhapter, Christian Maurer,
Stefan Bernet, and Monika Ritsch-Marte

Division for Biomedical Physics, Innsbruck Medical University, Müllerstrasse 44
A-6020 Innsbruck, Austria
Stefan.Bernet@i-med.ac.at

Abstract: We investigate holographic optical tweezers manipulating micro-beads at a suspended air-liquid interface. Axial confinement of the particles in the two-dimensional interface is maintained by the interplay between surface tension and gravity. Therefore, optical trapping of the micro-beads is possible even with a long distance air objective. Efficient micro-circulation of the liquid can be induced by fast rotating beads, driven by the orbital angular momentum transfer of incident Laguerre-Gaussian (doughnut) laser modes. Our setup allows various ways of creating a tailored dynamic flow of particles and liquid within the surface. We demonstrate examples of surface manipulations like efficient vortex pumps and mixers, interactive particle flow steering by arrays of vortex pumps, the feasibility of achieving a "clocked" traffic of micro beads, and size-selective guiding of beads along optical "conveyor belts".

© 2006 Optical Society of America

OCIS codes: (140.7010) Trapping, (090.1760) Computer holography, (170.4520) Optical confinement and manipulation.

References and links

1. E. R. Dufresne and D. G. Grier, "Optical tweezer arrays and optical substrates created with diffractive optical elements," *Rev. Sci. Instr.* **69**, 1974–1977 (1998).
2. M. J. Lang and S. M. Block, "Resource Letter: LBOT-1: Laser based optical tweezers," *Am. J. Phys.* **71**, 201–215 (2003).
3. J. Liesener, M. Reicherter, T. Haist, and H. J. Tiziani, "Multi-functional optical tweezers using computer-generated holograms," *Opt. Commun.* **185**, 77–82 (2000).
4. R. L. Eriksen, V. R. Daria, and J. Glückstad, "Fully dynamic multiple-beam optical tweezers," *Opt. Express* **10**, 597–602 (2002).
5. W. J. Hossack, E. Theofanidou, J. Crain, K. Heggarty, and M. Birch, "High-speed holographic optical tweezers using a ferroelectric liquid crystal microdisplay," *Opt. Express* **11**, 2053–2059 (2003).
6. P. T. Korda, M. B. Taylor, and D. G. Grier, "Kinetically locked-in colloidal transport in an array of optical tweezers," *Phys. Rev. Lett.* **89**, 128301 (2002).
7. M. P. MacDonald, G. C. Spalding, and K. Dholakia, "Microfluidic sorting in an optical lattice," *Nature* **426**, 421–424 (2003).
8. A. Jesacher, S. Fürhapter, S. Bernet, and M. Ritsch-Marte, "Size-selective trapping with optical cogwheel tweezers," *Opt. Express* **12**, 4129–4135 (2004).
9. D. G. Grier, "A revolution in optical manipulation," *Nature* **424**, 810–816 (2003).
10. K. Ladavac and D. G. Grier, "Microoptomechanical pumps assembled and driven by holographic optical vortex arrays," *Opt. Express* **12**, 1144–1149 (2004).
11. J. E. Curtis and D. G. Grier, "Structure of optical vortices," *Phys. Rev. Lett.* **90**, 133901 (2003).
12. V. Garcés-Chávez, K. Dholakia, and G. C. Spalding, "Extended-area optically induced organization of microparticles on a surface," *Appl. Phys. Lett.* **86**, 031106 (2005).

13. H. Melville, G. F. Milne, G. C. Spalding, W. Sibbett, K. Dholakia, and D. McGloin, "Optical trapping of three-dimensional structures using dynamic holograms," *Opt. Express* **11**, 3562–3567 (2003).
14. J. Leach, G. Sinclair, P. Jordan, J. Courtial, M. J. Padgett, J. Cooper, and Z. J. Laczik, "3D manipulation of particles into crystal structures using holographic optical tweezers," *Opt. Express* **12**, 220–226 (2004).
15. C. Bertocchi, A. Ravasio, S. Bernet, G. Putz, P. Dietl, and T. Haller, "Optical measurement of surface tension in a miniaturized air-liquid interface and its application in lung physiology," *Biophys J.* 2005 **89**, 1353–1361 (2005).
16. A. Jesacher, S. Fühapter, S. Bernet, and M. Ritsch-Marte, "Diffractive optical tweezers in the Fresnel regime," *Opt. Express* **12**, 2243–2250 (2004).
17. M. Polin, K. Ladavac, S. -H. Lee, Y. Roichman, and D. Grier, "Optimized holographic optical traps," *Opt. Express* **13**, 5831–5845 (2005).
18. E. R. Dufresne, G. C. Spalding, M. T. Dearing, S. A. Sheets, and D. G. Grier, "Computer-generated optical tweezer arrays," *Rev. Sci. Instrum.* **72**, 1810–1816 (2001).
19. K. Ladavac and D. G. Grier, "Colloidal hydrodynamic coupling in concentric optical vortices," *Europhys. Lett.* **70**, 548–552 (2005).
20. K. Ladavac and D. G. Grier, "Statistically Locked-in Transport Through Periodic Potential Landscapes," *Phys. Rev. Lett.* **92**, 130602(2004).
21. M.M. Burns, J.-M. Fournier, and J.A. Golovchenko, "Optical binding," *Phys. Rev. Lett.* **63**, 1233 (1989).
22. D. McGloin, A. E. Carruthers, K. Dholakia, and E. M. Wright, "Optically bound microscopic particles in one dimension," *Phys. Rev. E* **69**, 021403 (2004).
23. W. Singer, M. Frick, S. Bernet, and M. Ritsch-Marte, "Self-organized array of regularly spaced microbeads in a fiber-optical trap," *J. Opt. Soc. Am. B* **20**, 1568 (2003).

1. Introduction

Diffractive optical tweezers [1] have been demonstrated for various applications like flexible trapping and manipulation of microscopic particles [2, 3, 4, 5], sorting of particles in microfluidic flows [6, 7], size-selective particle trapping [8], or pumping and guiding particles by angular momentum transferring beams [9, 10, 11]. In most applications (one exception is described in [12]) the trapped particles are in a liquid environment, and trapping or guiding is performed in three dimensions (e.g. [13, 14]). For the purpose of three-dimensional trapping one has to use microscope objectives with a high numerical aperture, required mainly for particle confinement in the axial direction. Sufficiently high numerical apertures can only be obtained by using immersion objectives. Since the objectives are immersed in a liquid it is not possible to manipulate particles at a gas-liquid interface.

However, there are many interesting effects which can be studied at interfaces, for example the effects of surfactant, the assimilation of molecular monolayers at surfaces (Langmuir-Blodgett films), the effects of surface tension and exposure to air on biological samples like living cells, and local material parameters like surface viscosity and surface tension [15]. Particularly the effects of surface tension at such microscopic scales are of great importance, since this force dominates all other forces at micro-scales. Other interesting effects are surface convection which can be driven either by temperature- or by surfactant gradients within the surface. Therefore an optical tweezers system giving experimental access to such an interface can be a valuable tool for many new studies.

Here we present a diffractive optical tweezers setup acting at a well-defined microscopic gas-liquid surface. The surface is created in a specially designed vessel, consisting of a conical drill in a plastic disc (see photograph in Fig. 1). At the lower side, the plastic disc is pierced such that a circular opening with a diameter of 200 microns is formed. Liquid containing micro-beads, cells, etc. can be filled in from above, and the surface tension prevents the liquid from leaking through the tiny hole at the bottom. Thus, a well-defined micro-surface with a diameter of about 200 microns is formed at the bottom hole, which can be observed from below by an inverted microscope with an air objective. In order to manipulate particles at the inverted surface with laser tweezers, we use a holographically steered optical tweezers setup which is described in the following section.

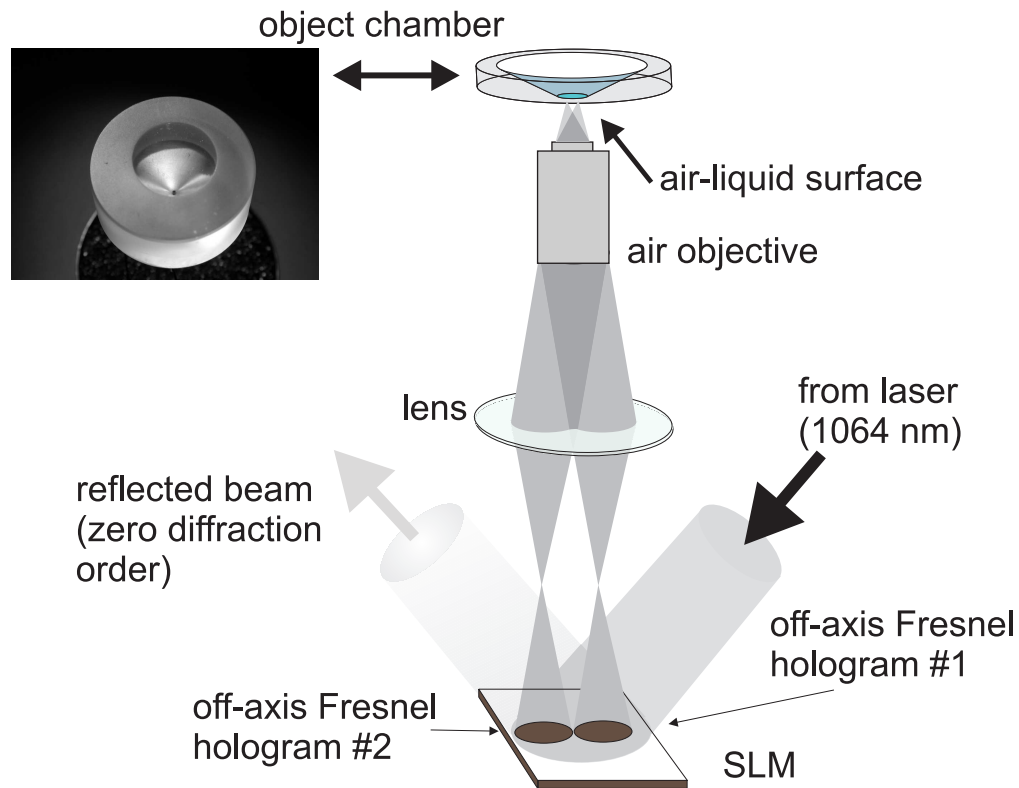


Fig. 1. Experimental setup for diffractive steering of optical tweezers at an inverted (“hanging”) air-liquid interface. A photograph of the object chamber is displayed at the upper left corner. The object chamber consists of a plastic disc of 1 cm height with a conical drill in its center. At the bottom the chamber has a circular opening with a diameter of about 200 microns. If the chamber is filled with a liquid, surface tension prevents leaking through the tiny hole. The air-liquid surface can be manipulated by optical tweezers from below by an inverted microscope. For the laser tweezers a high resolution (1920 x 1200 pixels) reflective spatial light modulator (SLM) is illuminated by an expanded collimated laser beam. At the SLM various image windows displaying computer-designed off-axis holograms (two examples displayed in the figure) are displayed. Only laser light diffracted from these holograms into the desired first order is guided by a lens to the rear input aperture of a microscope objective, and creates a programmed light field distribution at the air-liquid interface.

2. Experimental setup

A sketch of the setup is displayed in Fig. 1. An expanded laser beam emerging from an Ytterbium fiber laser (with a continuous wave emission at a wavelength of 1064 nm with an adjustable optical power of up to 10 W) is expanded and illuminates a high resolution spatial light modulator (SLM, 1920×1200 pixels with a pixel size of $10 \times 10 \mu\text{m}^2$). The polarization of the incoming light is adjusted such that the SLM acts as a phase shifter. The SLM is controlled by the graphics output of a computer and displays a copy of the "normal" graylevel monitor image as a phase image. Each pixel of the SLM can modulate the incoming light in a phase range between 0 and 1.4π (at the wavelength of 1064 nm) according to the corresponding gray levels of the displayed image. A further lens guides the light diffracted off the SLM to the rear input of a microscope objective. Finally, a non-immersion (air) microscope objective projects the desired optical field distribution onto the air-liquid surface. For our experiments we use either a 63 x Zeiss Achroplan (NA=0.95) or a 40 x Zeiss LD-Plan objective with a relatively low numerical aperture of 0.6, and a long working distance of 1.5 mm.

In the experiments described in section 4 ("arrays of vortex pumps") the SLM is positioned neither in a Fourier plane, nor in an image plane with respect to the sample surface, but instead in an intermediate Fresnel plane. This means, that the calculated field distributions are basically the Fourier transform of the desired image field, however with a superposed lens term and a linear phase shift to produce an off-axis hologram. Details of the hologram computation are explained in [16]. A great advantage of such a Fresnel setup as compared to normal Fourier setups (where the SLM is in a Fourier plane with respect to the sample plane) is that the projected image now depends on the spatial position of the hologram displayed at the SLM. For example, shifting a window on the SLM screen by mouse-dragging moves the corresponding light field distribution in the object plane. Furthermore, different holograms can be placed in different image windows at adjacent screen positions, which project independent image fields at selected parts of the sample plane. A second advantage of the Fresnel setup is the fact that undesired diffraction orders (and particularly the zero diffraction order, i.e. the specular reflection of the SLM) are suppressed since they are not sharply imaged into the object plane, but strongly out of focus. A similar, complementary setup in a Fresnel regime has been demonstrated in [17], however with converging illumination of the SLM, resulting in a focal spot of the zero diffraction order which was filtered out with an aperture stop.

The holographic steering of the laser beam can be used to create optical traps by focussed spots [18], or more sophisticated light fields like Laguerre-Gauss ("doughnut") modes [11], or whole arrays of such beams [10]. If particles (like micro-beads) within the liquid reach the air-liquid surface, they are held within the surface by surface tension. Thus optical tweezers can trap and move the particles within the two-dimensional surface without the need of axial confinement. This is the reason why air-objectives with their rather low numerical aperture can be used, since a high numerical aperture is only needed for axial trapping. In the following we investigate a toolbox of optical micro-manipulation methods which can be applied to trap and drive particles through such a surface.

3. Surface vortex pumps

In previous experiments it has been shown that Laguerre-Gaussian light modes can transfer orbital angular momentum to trapped particles. This results in a rotation of the particles around a doughnut shaped ring of light, even for static light fields. The rotational direction is adjusted by the sign of the helical index l of the doughnut beam. The diameter of the ring depends linearly on the helical index [11], l , which in our setup can be selected up to $l = 200$. Typically, the particles are trapped in the intensity maximum of the light ring within a two-dimensional plane, but three-dimensional (axial) trapping is not achieved due to an insufficient intensity

gradient in the axial direction. Therefore, for these experiments particles have to be confined in z-direction by another method. In other experiments [10, 19] this has been done by sandwiching a thin layer of liquid together with the particles between two glass coverslips with spacers on the order of 10 to 20 microns. Here we achieve the axial confinement directly within the air-liquid surface.

As a first demonstration of orbital angular momentum transfer to particles trapped at an air-water interface, a movie (Fig. 2) shows trapping and high speed rotation of multiple microbeads (with a size of $1.4\ \mu\text{m}$) in a doughnut mode with a helical index of 20.

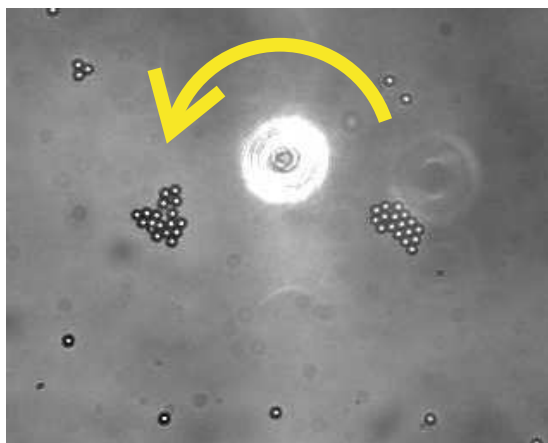


Fig. 2. (Movie fig2.avi 2.1 MB) High-speed rotation of multiple particles in a doughnut mode of helical index 20 induces a flow of the whole surface, as seen by the rotation of particles in the surroundings of the "vortex pump". The corresponding movie is displayed in real time.

In the example, the power of the trapping laser was adjusted to 9.6 W, corresponding to approximately 1.5 W of light power distributed along the ring circumference. The power reduction is mainly due to the limited diffraction efficiency of the SLM into the desired first diffraction order, and due to absorption within the microscope objective. The rotational velocity of the beads is on the order of 8 Hz, corresponding to a track speed of approximately 0.5 mm per second. Obviously the rotation of the trapped beads induces a rotational flow in the whole surface around the beads as demonstrated by some untrapped particles swirling around the central doughnut field. Obviously the vortex flow in the liquid surface decreases with increasing distance from the rotation center.

A possible application for the use of such a vortex pump could on the one hand be the measurement of surface viscosity and surface mobility of particles, and on the other hand to act as an efficient driving motor for creating surface flows which - for example - can be used for size-selective sorting of particles by guiding them through optical potential "landscapes" [20].

4. Arrays of vortex pumps

Another application of optical doughnut modes consists in the creation of programmable "conveyor belts" for the transport of micro-particles created by arrays of vortex pumps, as for example in [10]. A possible arrangement consists in multiple projected doughnut beams which can have different helical charges, and different signs of their helical indices. An example is shown in Fig. 3.

The figure shows a sequence of images from a movie, which demonstrate an interactively

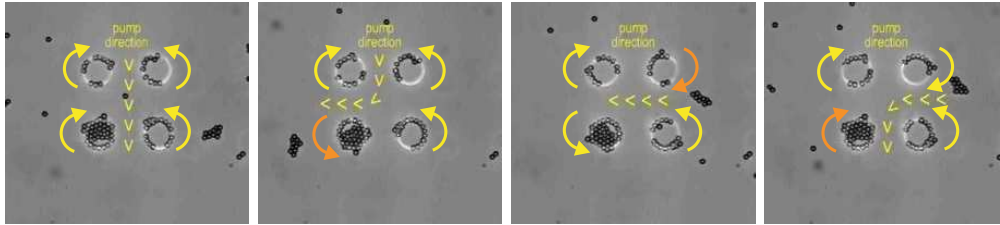


Fig. 3. (Movie fig3.avi 2.4 MB) Generation of surface flow into interactively selectable directions. Four doughnut modes with the same helical index but selectable rotation orientations (indicated by yellow and orange semicircles in the figures) are projected onto the surface. The light modes are "filled" with trapped beads which rotate into the selected directions and create a corresponding surface flow (direction of flow also indicated in the pictures by arrows). By changing the rotational direction of one of the doughnut modes from sequence to sequence (indicated by orange arrows) the surface flow can be controlled. This is demonstrated by the transport of unbound beads in the corresponding movie, which indicate the flow of the liquid in the surface.

steerable liquid flow in the surface. Four doughnut modes (each with a helical index of 20) are arranged in a square. Our Fresnel setup allows to create each of the doughnut modes *individually* by diffraction at a separate image window displayed at the SLM, i.e. the doughnut array is produced by a corresponding array of Fresnel holograms. Thus, the distance between the doughnut modes can be adjusted by mouse-dragging the corresponding hologram windows across the SLM screen. Furthermore, the helical index of each of the programmed doughnut modes can be easily and independently controlled by displaying the corresponding hologram or its mirror image. This allows to create a set of doughnut beams where the helicity of each doughnut can be switched individually, without calculating a novel hologram for the whole projected optical field.

In order to induce a surface flow, the doughnut modes are "loaded" by trapped beads. The optically induced rotation of these beads generates a corresponding flow in the surrounding liquid. In the first part of the movie the four doughnut modes induce a particle rotation into the directions indicated by the arrows. The flow profile can be observed by the flow of unbound particles in the surrounding. Obviously, in the first part of the movie a flow from the upper to the lower direction along a line through the center of the doughnut array is induced. Switching the sign of helical index of one of the doughnut modes (indicated by the orange arrow in the second image of Fig. 3) changes the flow profile. Now a freely floating bead follows a bent path through the doughnut array, with a 90° turn in its center. Switching the signs of other doughnut beams results in repeated changes of the flow pattern as seen in the movie.

The method can be extended to get an efficient "mixer" of the surface liquid. For this purpose two concentrically arranged doughnut modes of different helical indices are projected at the surface, as shown in Fig. 4. In the experiment one smaller doughnut mode with a helical index of -20 is centered within a larger mode with an index of 35. Since the signs of the two helical indices are different, the rotational directions of beads trapped in the two corresponding light rings are opposite. The corresponding surface liquid flow induced by the two counter-rotating bead systems thus produces hydrodynamic vortices in the surface region between the two doughnut rings. Consequently such an arrangement of doughnut modes can act as an efficient mixer for minute amounts of liquid. In our experiment, the vortices are visualized by the mixing of a bunch of micro-beads being trapped in the region between the two light rings. A similar system of two concentric doughnut modes has been presented in [19] and been suggested as a measurement method for the viscosity of the liquid, for example by comparing the

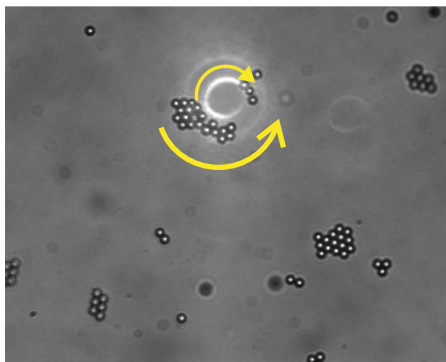


Fig. 4. (Movie fig4.avi 1.5 MB) Efficient mixing of fluid and particles trapped in a light field consisting of two concentric doughnut modes with different diameter and helicity, and two different signs of their respective helical indices. The particles trapped at the inner and outer light ring are rotating in opposite directions (indicated by yellow semi-circles in the figure), creating vortices of the liquid at the surface in the area between the two light rings. In the movie these vortices are demonstrated to mix a bunch of micro-beads in the area between the two circles.

rotational velocities of co- and counter-propagating micro-beads trapped by the two rings.

In Fig. 5 we present a modification of such a tool, which probes the flow of the liquid in the surface within a whole range of relative distances between the two light modes.

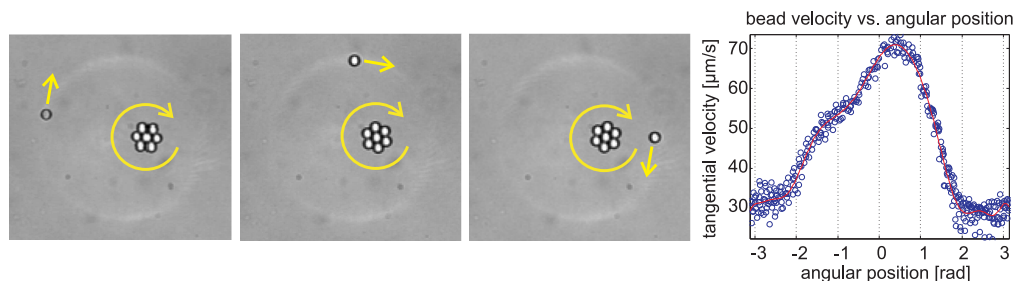


Fig. 5. (Movie fig5.avi 1.2 MB) Two doughnut modes with different helicities and different diameters are eccentrically arranged. The two helicities have the same sign, such that their induced rotations have the same orientations. The inner light ring is filled with beads, such that a surface flow is induced. The movie shows the hydrodynamic coupling between the vortex surface flow induced by the inner rotating ring of beads and the outer orbiting bead. The velocity of the single bead depends on its distance from the inner ring. The right inset is a plot of the tangential bead velocity as a function of its angular position. The closest distance between the two rings is obtained at the zero angle position. The plot shows that the maximal bead velocity is obtained before the bead actually reaches the zero angle position (note that the positive angle direction is measured counter-clockwise, whereas the beads rotate clockwise).

To this end the two doughnut modes are arranged similar as in the last experiment, but the doughnut rings are not concentric any more. As a consequence, beads rotating at the outer and inner rings have different relative distances at different positions on the rings, and their hydrodynamic interaction by the surface flow changes continuously. In principle, by tracking the particle movement of beads trapped at the inner and outer light rings, their hydrodynamic coupling induced by the viscosity of the surrounding liquid could be measured.

However, in our experiment we got the surprising result that the interaction between beads at the outer and inner ring is not purely hydrodynamic, but also affected by optical effects. In the experiment we "loaded" the inner ring with beads rotating in one direction. Since the inner ring was completely "filled" we expected the generation of a stationary surface flow. The corresponding flow profile was probed by a single bead rotating on the excentrically arranged outer ring into the same direction as the inner beads. By measuring the tangential velocity of the outer bead by video-tracking software we made the observation that the local bead velocity was not symmetric with respect to the symmetry axis of the two traps (i.e. the connection line between the centers of the two doughnut beams). Instead, the plot of the velocity as a function of the bead angular position (right insert of Fig. 5) shows that the velocity of the bead at the outer ring became maximal before reaching the closest approach between the two rings, and it significantly decreased at the symmetric position behind the point of the closest approach. The experiment was repeated three times with similar results with different doughnut-generating holograms in order to exclude effects due to a possible non-uniformity of the light intensity distributions. We also excluded an electrostatic interaction (rejection of beads with equal charge) by adding salt ions to the liquid. After exclusion of artifacts by a non-uniform intensity distribution, or an electrostatic interaction, an optical interaction seems the most plausible explanation.

In fact, the beads move within a light interference pattern which is created by the incoming light and the light scattered by the beads themselves. It has been shown in previous work, that such interferences lead to a complicated optically induced interaction between the beads, which is also denoted sometimes as "optical binding" [21, 22, 23]. There, beads are moving in a light potential which is strongly influenced by the beads themselves. In static light fields without orbital angular momentum transfer, this results in a static arrangement of beads such that the coupled system of beads and light field is in a minimum of its potential energy. In our actual case, the effects of this optically induced interaction may for the first time be examined in a dynamical system. There the interaction leads to deviations of the particle velocities from their expected values when approaching each other. In fact, the movie of Fig. 5 shows that moving fringes are generated by the interference of light scattered from the travelling outer bead with the incident projected light field. Thus it can be assumed that moving beads generate moving optical interference patterns which can trap and move other adjacent particles, thus inducing an optically transferred particle interaction based on the interference of scattered light.

Further evidence for this assumption is demonstrated in the experimental results presented in the movie of Fig. 6. There a bead circling at the outer doughnut ring is at a certain position completely stopped by the counter-rotating hydrodynamic flow induced by beads swirling in the inner, excentrically arranged ring. However, as soon as a second bead (which also moves at the outer ring) approaches the first one to a distance of approximately 11 microns, corresponding to 4 bead diameters, an apparent repulsive interaction between the two beads at the outer ring releases the stationary bead from its trap such that it proceeds with its path along the outer ring. In the following, the other bead approaches the trapping position and gets trapped itself, exchanging the roles of trapped and released beads. This sequence continues periodically. The movie demonstrates the existence of a long-range interaction between the two micro-beads in the outer ring, which is probably induced by optical forces due to scattered light. A more detailed theoretical treatment of this interaction is beyond the scope of the present article, but will be performed in the future together with further experimental investigations of this phenomenon.

5. Clocked bead traffic

The previous experiment has demonstrated that one particle in a "stopped" position can be released by an approaching second one. If such a situation could be extended to an arrangement

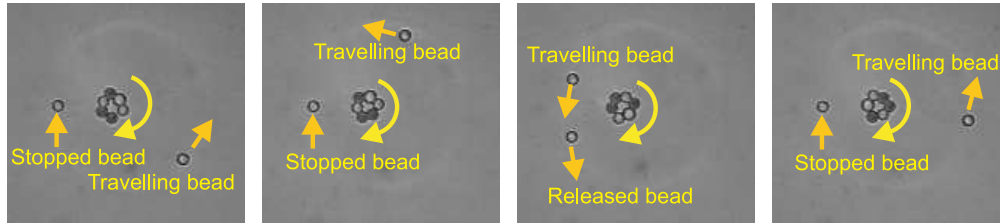


Fig. 6. (Movie fig6.avi 2.5 MB) Long range interaction of beads moving in a light field and a hydrodynamic flow field induced by a rotating vortex pump (center). Two beads are trapped in the light potential of an outer doughnut ring which induces a counter-clockwise rotation. However, an inner ring filled with beads induces a clockwise surface flow. At a certain position one of the two outer beads is stopped due to a balance between the counter-clockwise acting optical scattering force and the clockwise acting surface flow. However, the bead is released from its equilibrium position as soon as the second bead approaches to a distance of several bead diameters. In the following, the two beads change their roles, i.e. the travelling bead becomes trapped, whereas the formerly trapped bead advances around the orbit. The whole movement repeats periodically, as can be seen in the attached movie.

of multiple beads and multiple "stopping" positions, this would result in a "clocked" traffic of beads that could be used for a synchronization in the processing of multiple particles. For example, one particle is kept waiting until another particle, which is released elsewhere, pushes it out of its trap. A first step for the realization of such a timing between particle transport is demonstrated the experiment presented in Fig. 7.

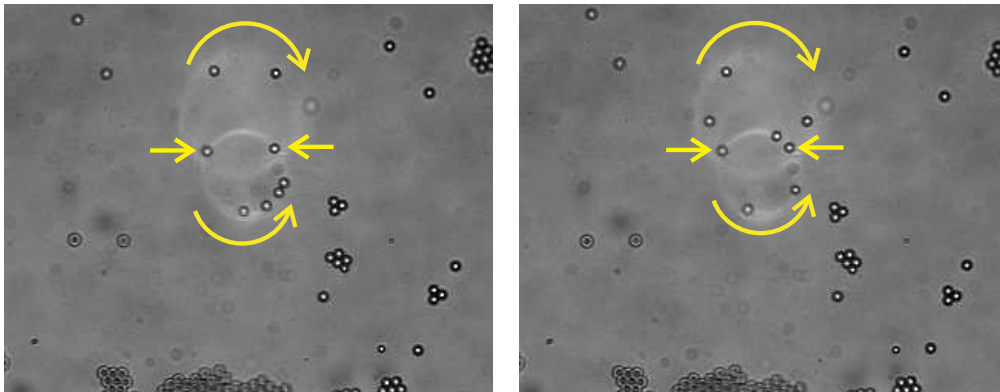


Fig. 7. (Movie fig7.avi 1.3 MB) Clocked bead traffic. Beads are orbiting at two intersecting doughnut modes of different helicities and rotational directions (indicated by yellow semi-circles). The two intersection points (indicated by arrows) are stable traps for beads. The movie shows that the trapped beads are pushed away by other beads circling around the doughnut modes, which subsequently get trapped themselves.

There two intersecting doughnut modes of different helicity are arranged such that they cross at two positions. The intersection points are stable trapping positions for beads, since they are local maxima of the light intensity. In the experiment demonstrated in the movie of Fig. 7, there are various beads moving at the two doughnut modes. Beads which reach the intersection points are stably trapped. However, they are released as soon as another bead arrives which pushes them out of their stable position and gets trapped itself. In this case, the originally trapped bead proceeds on the same ring and into the same direction from which its "rescuer"

approached. As a result, a complicated "traffic" of beads arises, redistributing them between the two storage rings. For future applications, such a clocked bead traffic might be used in different contexts, like producing a controlled interaction between beads coated with different substances. For example, if the two rings were loaded with beads of two different types, then each bead which changes from one ring to the other has interacted with a bead from the other species. The method can be extended to include a larger number of intersecting doughnut rings which provide the possibility to control the interactions between various bead species which may carry different chemical or biological substances.

6. Size-selective splitting of particle pathways

Selection of beads according to different properties such as size can be of advantage for various types of applications [7, 6, 8]. Here we demonstrate that the path a bead chooses in a specially tailored arrangement of optical "conveyor belts" can depend on its size. In our example (Fig. 8) two excentric doughnut modes are arranged close to each other, such that they almost touch tangentially at the position of their closest distance.

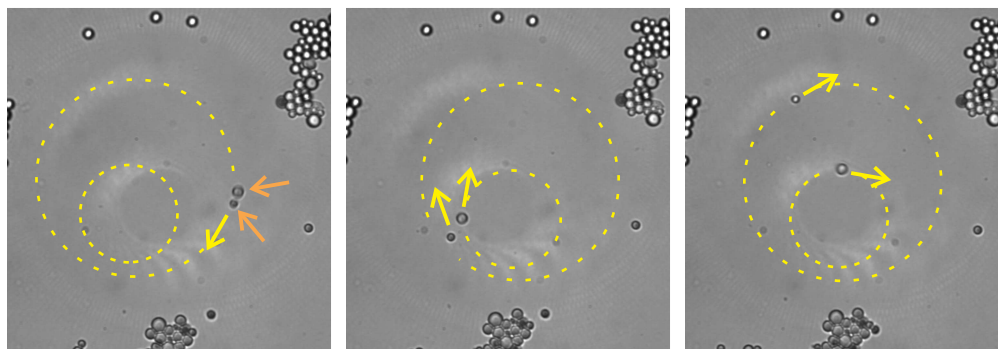


Fig. 8. (Movie fig8.avi 1.9 MB) Size selective splitting of the paths of micro beads. The movie shows two beads of different sizes (indicated by orange arrows) circling around a doughnut mode with a high helical index of 80 (indicated by the outer dashed yellow circle). As the beads approach an excentrically arranged inner light ring (doughnut mode with a helical index of 30) the larger bead is drawn into the inner circle, whereas the smaller bead proceeds on its orbit on the outer circle.

The two doughnut modes have helicities of 80 and 30, respectively, and they have a distance of approximately $1 \mu\text{m}$ at the point of the closest approach. The liquid contains a mixture of beads with two different diameters of 2 and $1.4 \mu\text{m}$, respectively. The beads are first trapped in an orbit around the outer doughnut ring. As they approach the point of the nearest distance between the two doughnut rings, only beads which are large enough to come into contact with the light field of the inner ring are drawn to this ring, whereas smaller beads stay on their orbit on the outer ring. The transition of the large beads from the outer to the inner ring is due to the larger light intensity and larger potential curvature of the inner ring due to the narrower localization of the light energy in smaller doughnut rings. Therefore the depth of the gradient potential produced by the inner ring is deeper than that of the outer ring, favoring the transition of the beads to the inner ring. The movie shows a small bead (size: $1.4 \mu\text{m}$) travelling around the outer ring, being not influenced by the potential of the inner one which is too far away, thus it stays on its orbit. The small bead is followed by a larger one (size $2 \mu\text{m}$) which is drawn to the inner one as soon as it approaches the point of the nearest distance between the two orbits.

The experiment is an example of a size-selective pathway splitter for micro-beads, which

will probably also work for biological objects like cells. An extension of the demonstrated principle is possible, for example, by creating pathways which split at various positions, where the distance between the splitting pathways decreases from one crossing to the next. Such an arrangement could be used for a fractional sorting of a mixture of particles with various sizes.

7. Summary

The present article intends to give an overview on optical manipulation methods of a gas-liquid surface which are realized by holographic methods. Some of the presented results (like vortex pumps and vortex arrays) have been already reported previously by other groups, however the main difference of the present experiments are the application to interfaces, with the advantage of using air-objectives which may have a rather low numerical aperture for trapping of the particles in the two-dimensional surface. Thus the presented methods give access to the measurement of surface properties like viscosity and surface tension, which are of particular interest, since there they are dominant forces on a micro-scale. Most of the presented experiments make use of the fact that even static light fields can transfer orbital angular momentum to micro-particles within the surface, thus inducing a controlled surface flow. The applications range from highly efficient vortex pumps, which are able to set the whole surface into rotation, to efficient mixers using concentric counter-rotating doughnut fields, and to steerable flows generated by vortex arrays consisting of individually and interactively switchable doughnut modes. The experiments also demonstrate that the combination of intersecting doughnut modes leads to stable trapping positions, which can produce complicated "clocked" traffic of beads. Finally, the pathways of beads on their light guides can be split depending on their sizes. The individual (and - if desired - interactive) manipulation of different light traps is significantly simplified by using a Fresnel setup instead of a commonly used Fourier setup for holographic beam steering. Thus, the demonstrated toolbox of laser-tweezers may be a first step into the realization of an optical micro-workshop dealing with the selection, transport, and assembly of micro-structures at a gas-liquid interface.

Acknowledgments

The authors want to thank Thomas Haller (Department for Physiology and Medical Physics, Innsbruck Medical University) for the invention and fabrication of the "inverted surface object chamber". This work was supported by the Austrian Academy of Sciences (A.J.), and by the Austrian Science Foundation (FWF) Project No. P18051-N02.